Temperature and cryoprotectant influence secondary quinone binding position in bacterial reaction centers

P. Raj Pokkuluri, Philip D. Laible, Adam E. Crawford, Joy F. Mayfield, Mohammed A. Yousef, Stephan L. Ginell, Deborah K. Hanson, Marianne Schiffer*

Biosciences Division, Argonne National Laboratory, 9700 S. Cass Avenue, Argonne, IL 60439, USA

Received 1 April 2004; revised 10 June 2004; accepted 10 June 2004

Available online 2 July 2004

Edited by Richard Cogdell

Abstract **We have determined the first de novo position of the secondary quinone Q_B in the *Rhodobacter sphaeroides* reaction center (RC) using phases derived by the single wavelength anomalous dispersion method from crystals with selenomethionine substitution. We found that in frozen RC crystals, Q_B occupies primarily the proximal binding site. In contrast, our room temperature structure showed that Q_B is largely in the distal position. Both data sets were collected in dark-adapted conditions. We estimate that the occupancy of the Q_B site is 80% with a proximal: distal ratio of 4:1 in frozen RC crystals. We could not separate the effect of freezing from the effect of the cryoprotectants ethylene glycol or glycerol. These results could have far-reaching implications in structure/function studies of electron transfer in the acceptor quinone complex because the above are the most commonly used cryoprotectants in spectroscopic experiments.**

Keywords: Reaction center structure; X-ray diffraction; Single wavelength anomalous dispersion; Selenomethionine; Quinone; Cryoprotection

1. Introduction

The photosynthetic reaction center (RC) is a transmembrane complex that sequesters ten cofactors [1]. An iron–ligand complex connects the binding sites of ubiquinone (UQ) molecules that are the terminal electron acceptors, Q_A and Q_B. Electron transfer from Q_A^- to Q_B is conformationally gated [2–4] and ceases upon freezing of the RC [2,5].

In structures of wild-type and mutant RCs from two different species [6–15], it is clear that Q_B can occupy at least two different positions: (A) a binding site in which the ubiquinone headgroup is proximal to the Fe^{+2} atom and the O4 carbonyl atom forms a hydrogen bond with L190His (a ligand of the Fe^{+2} atom), and (B) a binding site where the headgroup is distal to the Fe^{+2} and is unable to form a hydrogen bond with L190His (Fig. 1). The two binding positions overlap to some extent and differ by a 180° rotation of the headgroup around its isoprenoid tail. Structural studies of the two quinone binding sites suggested that Q_B may move from the distal to proximal position upon exposure of the complex to light and that electron transfer from Q_A^- to Q_B occurs only when Q_B is in the proximal position [11]. These observations led to the hypothesis – now controversial – that the conformational gate for $Q_A^- \rightarrow Q_B$ electron transfer is rotation and movement of Q_B from the distal to the proximal binding site.

Two recent functional studies have refuted this hypothesis. In the first, optical time-resolved transient absorption experiments by Xu et al. [16] found that rates of $Q_A^- \rightarrow Q_B$ electron transfer are not affected by the length of the Q_B's isoprenoid tail, a factor that should influence its translation across a distance of ~4 Å (Fig. 1). In the second, FTIR results [17,18] suggest that neutral Q_B is bound in the proximal site and does not move from that position upon its reduction to a semiquinone. Further, computational studies have suggested that the position of Q_B is also influenced by pH [19]; it was found that Q_B is located in the distal site below pH 6.5 and in the proximal site above pH 9.

Structures obtained from trigonal crystals of *Rhodobacter* (*R.*) *sphaeroides* RCs grown from phosphate solution also suggest that factors other than light can influence the position of Q_B. It is bound in the proximal position in RCs carrying the A(M260)W mutation close to Q_A [20], the E(L212)A-D(L213)A mutations near Q_B [15], and the P(L209)Y mutation that is 9 Å from Q_B [14]. In RCs carrying other substitutions of L209Pro, Q_B is bound in the distal site in the P(L209)E mutant and in an intermediate location in the P(L209)F mutant [14]. In several structures derived from data collected at room temperature from wild-type RCs and RCs carrying mutations on the periplasmic side of the complex near the primary donor, the electron density for Q_B – albeit poor – suggests that the majority of it is present in the distal position [9,12,15,21]. The only exception was that Q_B is found to be proximal in the structure derived from a data set that was collected from a frozen crystal; this RC carried mutations near the primary donor [22].

In this study, we report conditions for freezing trigonal *R. sphaeroides* RC crystals and explore the effects of freezing and cryoprotectant on Q_B's binding position. In contrast to our room temperature structure [15] and the structure of the dark-adapted RC obtained from frozen tetragonal crystals [11], the position of Q_B in our frozen crystals was found to be proximal.

We also determined, for the first time,[1] the position of Q_B in a de novo, unbiased electron density map of the *R. sphaeroides*

* Corresponding author. Fax: +1-630-252-3387.
E-mail address: mschiffer@anl.gov (M. Schiffer).

[1] The original structure of the bacterial RC was that from *Rhodopseudomonas viridis* (now *Blastochloris* (*B.*) *viridis*); and was solved using heavy atom derivatives and the multiple isomorphous replacement method [1]. The structure of the *R. sphaeroides* RC solved via molecular replacement with the *B. viridis* RC as the search model [7,8] followed several years later.

0014-5793/$22.00 © 2004 Published by Elsevier B.V. on behalf of the Federation of European Biochemical Societies.
doi:10.1016/j.febslet.2004.06.042

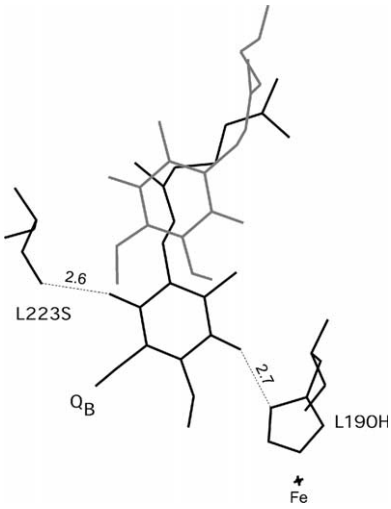

Fig. 1. The position(s) of Q_B in the structures of the *R. sphaeroides* RC. Distal site, gray ([15]; PDB code 1k6l; 298 K); proximal site, black (this study, SAD1 map; 100 K). The non-heme Fe^{2+}, L223Ser and L190His are also shown.

RC; experimental phases were derived from the single wavelength anomalous dispersion (SAD) method [23] at 100 K with crystals grown from selenomethionine-substituted protein. Consistent with our frozen data, the electron density showed that Q_B is largely bound in the proximal position.

2. Materials and methods

2.1. Preparation of crystals

Native, polyhistidine-tagged RCs were purified and crystallized with minimum light exposure as described previously [15]. Methionine residues of the RC were replaced by biosynthetic incorporation of selenomethionine (SeMet; P.D. Laible, A.N. Hata, A. Crawford, and D.K. Hanson, unpublished). The incorporation of SeMet was quantitative. The purification and crystallization of the SeMet protein was the same as that for the native RC.

2.2. Cryoprotection and data collection

RC crystals grown from phosphate solution were cryoprotected for data collection at first by serial transfer through 1.6 M potassium phosphate (pH 7.5) solution containing 5%, 10%, 15%, 20%, 25% and 28% ethylene glycol (data sets WT and SAD1); subsequently, we found that they could be soaked directly in cryosolution containing 28% ethylene glycol (SAD2) or 25% glycerol. In all cases, crystals were frozen within 2 min following transfer to cryosolution. The addition of cryoprotectant did not change the pH of the 1.6 M potassium phosphate solution. At the Advanced Photon Source (APS), cryoprotected crystals were flash-cooled by plunging into liquid nitrogen and data were collected at 100 K (WT, SAD1 and SAD2). For data collection on the rotating anode (Rigaku R-axis IIc) at 119 K, crystals were frozen in a cold nitrogen stream after a brief soak in 25% ethylene glycol or glycerol. As done previously [15], room temperature data were collected with crystals mounted in a quartz capillary using low intensity white light from a microscope; the WT and SAD1 data sets were collected on crystals that were exposed to relatively bright white light during manipulation on a microscope. The crystal used for the SAD2 data set was handled on a microscope fitted with a green filter and low light intensity was used to minimize the excitation of RCs in the crystal. During all data collections the crystals were kept in dark. The WT data set was collected on the 19BM beamline, and the SAD1 and SAD2 data sets were collected on the 19ID beamline (APS). Data collected at the APS were processed with HKL2000 [24] and R-Axis IIc data sets were processed with DENZO [24] and SCALEPACK [24].

2.3. Structure determination

Crystallographic parameters are summarized in Table 1. The WT structure at 100 K was solved by rigid-body refinement using the room temperature structure published previously ([15]; PDB code: 1k6l) with Q_B atoms removed as a search model. The SAD1 and SAD2 structures at 100 K were solved by using the SAD method with the program CNS [25] using the Se peak data.

2.4. Calculated quinone electron densities

For the calculation of electron density maps, UQ_{10} (truncated to C_{19}) in the proximal or distal position was placed in a $(50\ \text{Å})^3$ unit cell in space group P1 with temperature factors for all atoms set at 40 Å^2. The Q_B coordinates from the room-temperature wild-type RC structure ([15]; PDB code: 1k6l) were used as distal Q_B and the Q_B coordinates fitted to the SAD1 map were used as proximal Q_B. Electron density maps were then computed based on calculated structure factors using the program CNS [25].

3. Results and discussion

3.1 Effect of freezing and/or cryoprotectants on the position of Q_B

Table 1 shows the crystallographic data for the WT structure at 2.4 Å determined from a frozen trigonal crystal at 100 K with 28% ethylene glycol as a cryoprotectant. Preliminary ex-

Table 1
Crystallographic parameters for the WT and the SeMet RC crystals at 100 K

	WT	SAD1	SAD2
Space group	$P3_121$	$P3_121$	$P3_121$
Unit cell dimensions (Å)			
$a = b$	139.2	139.3	139.0
c	184.4	184.2	183.7
High resolution (last shell) (Å)	2.40 (2.49–2.40)	2.8 (2.9–2.8)	2.95 (3.06–2.95)
R_{merge} (last shell) (%)	4.3 (35.4)	7.6 (31.7)	6.7 (35.3)
$I/\sigma(I)$ (last shell)	27.4 (3.0)	18.9 (3.7)	28.0 (5.5)
Completeness (last shell) (%)	98 (95)	99 (98)	100 (100)
Redundancy (last shell)	3.6 (2.5)	3.5 (3.2)	3.6 (3.7)
Data collection wavelength (Å)	0.97926	0.97910	0.97948
SAD phasing (CNS)			
Figure of merit (FOM)	–	0.30	0.34
FOM after solvent modification	–	0.96	0.96
Light used for crystal mounting	White	White	Green
Major Q_B position	Proximal	Proximal	Proximal

amination of the structure shows that it is in good agreement with that derived at room temperature [15] with the exception of the boundaries of the molecules affected by the shrinkage of the unit cell at 100 K, as has been observed for other structures [26]. These data show that the position of the quinone is affected greatly by the freezing process, although the surrounding protein residues are not. Q_B was bound in the distal position in the RC structure obtained from data that were collected at room temperature [15], whereas it is in the proximal position in the structure obtained from all frozen crystals reported herein.

Ethylene glycol versus glycerol for cryoprotection. To determine whether ethylene glycol itself is responsible for shifting Q_B to the proximal site, we also used glycerol as the cryoprotectant. Although, we found glycerol to be less effective than ethylene glycol in preserving the frozen RC crystal, the electron density derived from data at 3.5 Å also indicated that Q_B is bound in the proximal site (data not shown). Therefore, the shift of Q_B to the proximal position is not specific for either cryoprotectant.

The present data speak of the difficulty in determining the factors that affect the position of Q_B in structural studies. The freezing of RC crystals involved two processes: (A) addition of cryoprotectant and (B) lowering of the temperature. We were unable to determine which one of these two factors is responsible for shifting Q_B from the distal to the proximal position – collection of data at room temperature from RC crystals exposed to ethylene glycol and glycerol failed because the presence of even small amounts, 0.5%, of the additive destroyed the crystal lattice during the length of time (hours) required for the data collection, and it is impossible to obtain data from trigonal RC crystals frozen without cryoprotectant.

Ethylene glycol and glycerol are commonly used in low temperature spectroscopic measurements of electron transfer rates in the acceptor quinone complex (see e.g., [5,16]). While we cannot know whether these cryoprotectants have the same effects in solution as we have observed in the RC crystals, Tiede et al. [5] have demonstrated that the addition of ethylene glycol to native RC preparations affects both the rate and amplitude of the fast phase of transfer of the first electron to Q_B.

3.2. Advantages of phase determination by the SAD method

With conditions established for freezing of trigonal RC crystals, we could utilize the tunable X-ray source at the APS. The SAD method for phase determination exploits the anomalous scattering of an atom (e.g., Se) near the wavelength of its absorption edge [23]. In general, phases derived from molecular replacement suffer from ''phase bias'' in that the atomic model that is used to calculate the initial phases of the reflection data will influence the resulting electron density. To remove the model bias special techniques are required [27]; such refinement process can identify and remove possible errors in the model depending on the resolution and data quality. In contrast, electron density derived from de novo phase determination experiments – such as the SAD method – does not depend on an initial atomic model based on another structure, so no ''phase bias'' is introduced. Also, because of phase accuracy the electron density derived from SAD experiments is superior to that obtained by molecular replacement even in cases where the data resolution in the SAD data set is lower than that of data used in molecular replacement.

3.3. SeMet RC structure

We collected a full data set to 2.8 Å resolution at the K-absorption edge of Se (SAD1; Table 1). Selenium atoms in 22 of 24 substituted residues were found (two Met residues are in disordered regions of the RC structure). Electron density calculated after density modification is of excellent quality (FOM = 0.96; Table 1).

Our preliminary examination of the SAD map (refinement and full details of the SeMet RC structure will be published elsewhere) indicates that it is in good agreement with the published room temperature structures of *R. sphaeroides* RCs except at the boundaries of the molecule affected by the shrinkage of the unit cell. The unbiased, de novo electron density map obtained here indicated that Q_B was in a proximal position (Fig. 2A).

3.4. Effect of light on the position of Q_B

To rule out the possibility that the binding of Q_B in the proximal position in the frozen crystals may have been caused by the exposure of RC crystals to light from the microscope at the time of crystal manipulation before freezing, we collected a second SAD data set (SAD2; Table 1) with a crystal that was manipulated while using dim light from a microscope fitted with a green filter and frozen in the dark. These sub-saturating conditions limit the production and accumulation of charge-separated states in the opaque RC crystal. The electron density derived from the SAD2 data set also showed that Q_B was proximal; therefore, the exposure to the microscope light was not a factor in determining the position of Q_B in frozen crystals.

In both SAD data sets, the head and tail sections (to C_{19}) of the quinone are well defined. The electron density distribution

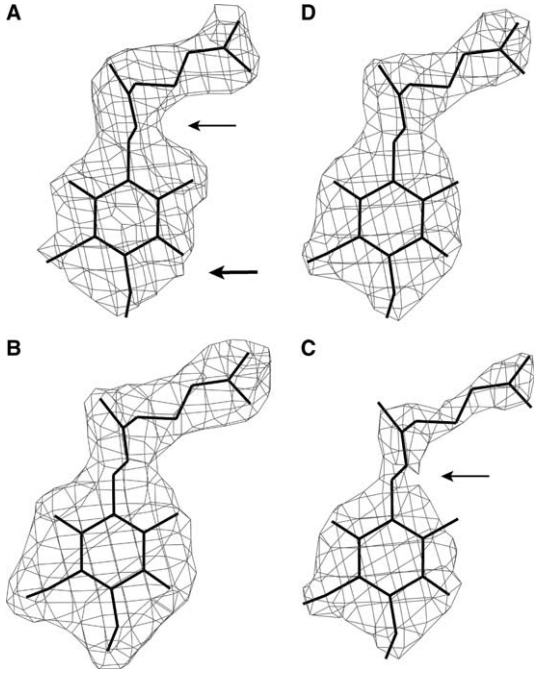

Fig. 2. Electron density maps for the Q_B site: (A) experimental map, SAD1 data set; calculated maps assuming occupancies of (B) 100% proximal, (C) 60% proximal, 0% distal, and (D) 64% proximal, 16% distal.

in the two structures is very similar; however, it suggested that the distal site may also be partially occupied.

3.5. Relative occupancies of the distal and proximal Q_B binding sites

Since Q_B represents only a very small fraction of the unit cell and the diffraction data are of medium resolution, the estimates of relative occupancy of the distal and proximal Q_B binding sites and their temperature factors that are obtained from the crystallographic refinement process tend to be unreliable. Therefore, to estimate the relative occupancies of the two Q_B binding sites in the experimental electron density, we calculated electron density maps that would result from set values for occupancies of the two sites. The calculated maps were then compared with the experimental electron density derived from the SAD1 data set. Those data are based on de novo phase information with no input from previously known RC structures and no assumptions about occupancies of any Q_B binding sites. In order to facilitate comparison of calculated and experimental maps, we found that the calculated map is needed to be contoured at 0.4 e/Å^3 so that the electron density of a quinone at 100% occupancy (Fig. 2B) reproduced that of Q_A in the SAD1 map contoured at 0.1 e/Å^3; the Q_A site is known to be fully occupied [28].

The SAD1 map was compared with the calculated maps by looking perpendicular to the face of Q_B bound at the proximal site. Since the distally bound quinone does not contribute to the "lower" part of the electron density (thick arrow, Fig. 2A), the comparison yields an estimate of about 60% occupancy for the proximal site (Fig. 2C). However, the electron density for Q_B in the SAD1 map was wider at its "neck" (thin arrow, Fig. 2A) and tail compared to the calculated map in Fig. 2C. Input parameters (proximal: distal ratio, total Q_B occupancy) were modified until improved agreement was reached between the calculated and experimental maps. This occurred when the total occupancy of the Q_B site was set at 80% and the proximal:distal occupancy ratio was set at 4:1 (64%:16%, Fig. 2D). The comparisons also suggested that the distal Q_B site in the frozen crystals is probably "lower" or more proximal than the distal Q_B observed in our room temperature RC structure [15].

3.6. Comparison with other RC structural data

Data presented here on the position of Q_B do not agree with those of Stowell et al. [11] and Fritzsch et al. [29]; they found that Q_B was bound mainly in the distal site when the RC crystals were frozen in the dark. Stowell et al. [11] reported that light exposure before flash cooling was required for binding of Q_B in the proximal site. Fritzsch et al. [29] also found that Q_B is bound mainly in the proximal site only after the RC crystals were exposed to light.

However, the experiments of these two groups cannot be directly compared with the experiments reported herein. Stowell et al. [11] used tetragonal crystals of the *R. sphaeroides* RC that were grown from PEG4000 and were frozen without additives. Fritzsch et al. [29] used a trigonal RC crystal grown from phosphate solution with 35% glycerol as the cryoprotectant and the RC crystal was reversibly flash-cooled four times (crystal annealing) before data collection. Another important difference may be that the other groups added UQ_2 to increase the occupancy of Q_B in their RC crystals. In comparison, our polyhistidine-tagged RCs were purified rapidly with affinity chromatography, a method that minimizes exposure of the RCs to high detergent levels that are known to decrease the occupancy of the Q_B site [5].

Acknowledgements: We thank Sam Hofman for technical expertise in preparing native RC crystals and Dr. David Tiede for helpful discussions. This work was supported in part by the National Institutes of Health (R01 GM61887 and R01 GM63849).

References

[1] Deisenhofer, J., Epp, O., Miki, K., Huber, R. and Michel, H. (1984) J. Mol. Biol. 180, 385–398.
[2] Kleinfeld, D., Okamura, M.Y. and Feher, G. (1984) Biochemistry 23, 5780–5786.
[3] Graige, M.S., Feher, G. and Okamura, M.Y. (1998) Proc. Natl. Acad. Sci. USA 95, 11679–11684.
[4] Li, J., Takahashi, E. and Gunner, M.R. (2000) Biochemistry 39, 7445–7454.
[5] Tiede, D.M., Vazquez, J., Cordova, J. and Marone, P.A. (1996) Biochemistry 35, 10763–10775.
[6] Deisenhofer, J., Epp, O., Miki, K., Huber, R. and Michel, H. (1985) Nature 318, 618–624.
[7] Allen, J.P., Feher, G., Yeates, T.O., Komiya, H. and Rees, D.C. (1987) Proc. Natl. Acad. Sci. USA 84, 5730–5734.
[8] Chang, C.-H., El-Kabbani, O., Tiede, D.M., Norris, J.R. and Schiffer, M. (1991) Biochemistry 30, 5352–5360.
[9] Ermler, U., Fritsch, G., Buchanan, S.K. and Michel, H. (1994) Structure 2, 925–936.
[10] Arnoux, B., Gaucher, J.F., Ducruix, A. and Reiss, F. (1995) Acta Crystallogr. D 51, 368–379.
[11] Stowell, M.H.B., McPhillips, T.M., Rees, D.C., Soltis, S.M., Abresch, E. and Feher, G. (1997) Science 276, 812–816.
[12] McAuley-Hecht, K.E., Fyfe, P.K., Ridge, J.P., Prince, S.M., Hunter, C.N., Isaacs, N.W., Cogdell, R.J. and Jones, M.R. (1998) Biochemistry 37, 4740–4750.
[13] Lancaster, C.R.D. (1999) Biochem. Soc. Trans. 27, 591–596.
[14] Kuglstatter, A., Ermler, U., Michel, H., Baciou, L. and Fritzsch, G. (2001) Biochemistry 40, 4253–4260.
[15] Pokkuluri, P.R., Laible, P.D., Deng, Y.L., Wong, T.N., Hanson, D.K. and Schiffer, M. (2002) Biochemistry 41, 5998–6007.
[16] Xu, Q., Baciou, L., Sebban, P. and Gunner, M.R. (2002) Biochemistry 41, 10021–10025.
[17] Breton, J., Boullais, C., Mioskowski, C., Sebban, P., Baciou, L. and Nabedryk, E. (2002) Biochemistry 41, 12921–12927.
[18] Nabedryk, E., Breton, J., Sebban, P. and Baciou, L. (2003) Biochemistry 42, 5819–5827.
[19] Taly, A., Sebban, P., Smith, J.C. and Ullmann, G.M. (2003) Biophys. J. 84, 2090–2098.
[20] McAuley, K.E., Fyfe, P.K., Ridge, J.P., Cogdell, R.J., Isaacs, N.W. and Jones, M.R. (2000) Biochemistry 39, 15032–15043.
[21] Fyfe, P.K., McAuley-Hecht, K.E., Ridge, J.P., Prince, S.M., Fritzsch, G., Isaacs, N.W., Cogdell, R.J. and Jones, M.R. (1998) Photosynth. Res. 55, 133–140.
[22] Fyfe, P.K., Ridge, J.P., McAuley, K.E., Cogdell, R.J., Isaacs, N.W. and Jones, M.R. (2000) Biochemistry 39, 5953–5960.
[23] Wang, B.C. (1985) Methods Enzymol. 115, 90–112.
[24] Otwinowski, Z. and Minor, W. (1997) Methods Enzymol. 276, 307–326.
[25] Brunger, A.T. et al. (1998) Acta Crystallogr. D 54, 905–921.
[26] Juers, D.H. and Matthews, B.W. (2001) J. Mol. Biol. 311, 851–862.
[27] Hodel, A., Kim, S.-H. and Brunger, A.T. (1992) Acta Crystallogr. A 48, 851–858.
[28] Wraight, C.A. (2004) Front. Biosci. 9, 309–337.
[29] Fritzsch, G., Koepke, J., Diem, R., Kuglstatter, A. and Baciou, L. (2002) Acta Crystallogr. D 58, 1660–1663.